EPJ manuscript No.
(will be inserted by the editor)

Thermal Dileptons from Coarse-Grained Transport as Fireball Probes at SIS Energies

Tetyana Galatyuk[1,2], Paul M. Hohler[3], Ralf Rapp[3], Florian Seck[1,2] and Joachim Stroth[3,2]

[1] Technische Universität Darmstadt, 64289 Darmstadt, Germany
[2] GSI Helmholtzzentrum für Schwerionenforschung GmbH, 64291 Darmstadt, Germany
[3] Texas A&M University, College Station, TX 77843-3366, USA
[4] Institut für Kernphysik, Goethe-Universität, 60438 Frankfurt, Germany

arXiv:1512.08688v2 [nucl-th] 18 May 2016

Abstract. Utilizing a coarse-graining method to convert hadronic transport simulations of Au+Au collisions at SIS energies into local temperature, baryon and pion densities, we compute the pertinent radiation of thermal dileptons based on an in-medium ρ spectral function that describes available spectra at ultrarelativistic collision energies. In particular, we analyze how far the resulting yields and slopes of the invariant-mass spectra can probe the lifetime and temperatures of the fireball. We find that dilepton radiation sets in after the initial overlap phase of the colliding nuclei of about 7 fm/c, and lasts for about 13 fm/c. This duration closely coincides with the development of the transverse collectivity of the baryons, thus establishing a direct correlation between hadronic collective effects and thermal EM radiation, and supporting a near local equilibration of the system. This fireball "lifetime" is substantially smaller than the typical 20-30 fm/c that naive considerations of the density evolution alone would suggest. We furthermore find that the total dilepton yield radiated into the invariant-mass window of $M = 0.3 - 0.7$ GeV/c^2 normalized to the number of charged pions, follows a relation to the lifetime found earlier in the (ultra-) relativistic regime of heavy-ion collisions, and thus corroborates the versatility of this tool. The spectral slopes of the invariant-mass spectra above the ϕ-meson mass provide a thermometer of the hottest phases of the collision, and agree well with the maximal temperatures extracted from the coarse-grained hadron spectra.

PACS. 25.75.Cj Dilepton production – 24.10.Lx Monte Carlo simulations – 24.10.Cn Many-body theory

1 Introduction

Lepton pairs have proven to be a formidable tool to probe the properties of extreme states of QCD matter as formed in reactions of heavy ions at (ultra-) relativistic energies [1]. Since electromagnetic (EM) probes decouple from the hot and dense interaction region once they are produced, their phase space distributions carry information about the temperature, collectivity and spectral structure of the QCD medium [2]. The recorded spectra are a space-time integral of a local, time-dependent emissivity of matter over the full reaction volume. The emissivity characterizes the radiation rate of (virtual) photons off a cell of strongly interacting matter per unit time and 4-momentum, $\epsilon = dN_{\rm ee}/dVdtd^4q$. In thermal equilibrium it depends on intensive medium properties such as temperature, density and chemical composition, and can be represented by the thermal average of the in-medium EM current-current correlator [3–5], $\epsilon = {\rm const} f^B(q_0,T)\rho_{\rm EM}/M^2$, where M is the invariant dilepton mass and f^B the thermal Bose distribution. In the vacuum, and at low masses, the EM spectral function $\rho_{\rm EM}$, is saturated by the decays of the light vector mesons ρ, ω and ϕ, while at very high temperatures (or high masses) it is characterized by the annihilation of weakly interacting quarks and antiquarks. A key objective of using dilepton emission is to study the modifications of hadron properties in a QCD medium and how these can signal the transition to deconfined and/or chirally restored phases of matter [1, 6, 7].

An important aspect in understanding dilepton radiation off matter under extreme conditions is the excitation function as the energy of the colliding nuclei is varied. On the one hand, this allows to vary the chemical composition of the system and to scan how hadron properties change across the QCD phase diagram, *i.e.*, to study the microphysics encoded in the EM emissivity. On the other hand, if one has control over the EM spectral function, one can utilize

Correspondence to: f.seck@gsi.de

dileptons to study the macrophysics of the fireball, as their spectra are determined by an interplay of the fireball's lifetime and volume with the strong (exponential) temperature dependence in the Bose distribution of the emissivity. Long lifetimes and large fireball volumes are typically associated with the later emission stages while a high temperature enhances the yields from the early phases. To study this interplay over the full range of collision energies, special care has to be taken in the modeling of the evolution of the reaction volume. At ultrarelativistic collision energies (CERN/SPS, BNL/RHIC and CERN/LHC) the source is believed to be close to local equilibrium and produce most of its entropy very quickly (within about 1 fm/c), forming a system of extreme energy density in the deconfined phase. It subsequently cools through rapid expansion and, after $\tau_{\rm QGP} \simeq 5-10$ fm/c, crosses over to a hadronic medium at a temperature of about 160 MeV, followed by a further expansion of $\tau_{\rm had} \simeq 5-10$ fm/c until thermal freeze-out at $T_{\rm fo} \simeq 100-120$ MeV. In this energy regime the observed dilepton spectra [8–13] can be understood using isentropically expanding fireballs or hydrodynamic models for the bulk medium evolution [14–19].

At the relativistic energies of LBNL/BEVALAC and GSI/SIS18 the situation is different. The Lorentz contraction of the incoming nuclei is moderate, and it already takes around 7 fm/c for two heavy ions (Au) to fully penetrate. Microscopic transport calculations predict that the maximum density in the center of the interaction region of a central Au+Au collision at 1A GeV lab energy is reached about 10 fm/c after initial impact [20], and that the total fireball lifetime is around 25 fm/c. A long-standing question in this context is whether local thermalization occurs in these systems, and, if so, over which period in time [21, 22]. Thus, in lieu of thermal approaches, dilepton spectra at these energies [23–26] are commonly calculated using non-equilibrium transport models [27–35]. However, in view of the expected strong medium effects on the hadronic spectral functions, a full quantum treatment of the associated off-shell effects is challenging. From the experimental side, one can monitor the dilepton excess radiation beyond final-state decays as a function of nucleon participant number, $N_{\rm part}$; an excess yield scaling stronger than linear in $N_{\rm part}$ can serve as a measure of the number of Δ or ρ generations produced during the fireball evolution at SIS ("Δ-clock") [26] or SPS energies ("ρ-clock") [36, 37], respectively. However, medium effects on their spectral functions compromise this measure. A quantitative measure of the fireball lifetime has recently been put forward in the ultrarelativistic regime [2]: the dilepton excess radiation in the low-mass window of $M = 0.3-0.7$ GeV/c^2 turns out to accurately reflect the underlying lifetime of the thermal system, if medium effects in the ρ spectral function are included.

In the present paper we pursue similar ideas to probe fireball properties in the relativistic collision energy regime, using, however, different methods due to the above mentioned complications in defining a thermal system. Specifically, we will compute the time dependent emission of dileptons by applying a coarse-graining method to an underlying transport evolution, as first carried out in Ref. [38] at SPS energies and in recent work in Refs. [39, 40]). The basic assumption of this procedure is that the interactions in the system are strong enough so that, by averaging over many transport events of the same collision configuration, one can extract meaningful local temperatures and baryon densities in space-time. If this assumption is valid, one gains the key advantage of being able to compute dilepton radiation by using microscopically calculated equilibrium rates, thus retaining their full quantum-field theoretical (off-shell) properties. Our goal in doing so is to identify observables which can differentiate between effects of the emissivity and the space-time evolution. In particular, we differ from and go beyond the recent work in Ref. [40] in several respects. This includes technical aspects such as the extraction of the temperature (with quantitative error estimates and their manifestation in the resulting dilepton yields) and an improved determination of the pion fugacity factor figuring in the dilepton production rate. We furthermore exhibit novel insights, such as a strong correlation of the time evolution of dilepton emission with the build-up of collectivity in the fireball (which also serves as an independent means to assess the validity of the coarse-graining procedure) and quantifying the temperature(s) and lifetime of the fireball.

Our paper is organized as follows. In Sec. 2 we briefly review the coarse-graining procedure, our concrete implementation thereof, and specify the in-medium EM emissivity employed in the calculations. In Sec. 3 we discuss the extraction and results for the time evolution of the thermodynamic parameters in Au-Au collisions at SIS18. In Sec. 4 we analyze the time profile of dilepton radiation, extract a fireball lifetime and temperatures from various regions of the invariant-mass spectra, and discuss the results in a broader context of heavy-ion collisions at varying energies. We summarize and conclude in Sec. 5.

2 Coarse Graining of Hadronic Transport

Microscopic transport simulations of heavy-ion collisions aim at a description of the space-time evolution of the phase-space distributions of all strongly-interacting particles involved in the reaction. In the SIS18 energy regime, with lab energies of up to a few A GeV, the calculations are usually performed using hadronic degrees of freedom. For each heavy-ion collision event, a complete reaction history of the positions and momenta of hadrons is computed, from the initial encounter of the two incoming nuclei until the final state when the interactions have ceased, by simulating the Boltzmann equation with suitable cross sections. Dilepton emission is commonly computed by integrating the dilepton branching ratio in each time step for all hadrons and scattering events. This is repeated for many events in a given

event class (*e.g.*, centrality) to obtain the average dilepton spectrum per event. However, the implementation of in-medium effects, in particular the treatment of hadrons with broad spectral distributions, remains rather challenging, see, *e.g.*, Refs. [41–43]. On the other hand, the use of hydrodynamics at relativistic energies also faces significant issues, most notably the timescales and justification of thermalization given the rather long penetration times of the incoming nuclei [44].

As a middle ground between the microscopic transport and macroscopic hydro approach a coarse-graining procedure has been suggested to compute the EM radiation of the interacting medium in heavy-ion collisions [38]. By averaging the pion and baryon distributions in suitable space-time cells over many events one extracts smooth space-time evolutions of temperature and chemical potentials in a given event class, which can be straightforwardly convoluted with a thermal dilepton emission rate. This combines the virtues of a microscopic space-time evolution with the benefits of thermal-field theoretically calculated in-medium dilepton rates. The price is the assumption of local thermal equilibrium in the extraction of temperature and chemical potentials, which, however, is mitigated compared to a full hydrodynamic simulation since deviations from the vanishing mean-free-path limit are still kept in the evolution (and, in fact, are also inherent in the dilepton rates).

The expression for the event-averaged 4-momentum differential dilepton emission spectrum is given as the space-time integral of the emissivity as

$$\left\langle \frac{\mathrm{d}N_{l^+l^-}}{\mathrm{d}y\mathrm{d}p_t\mathrm{d}M} \right\rangle = \int \frac{\mathrm{d}\epsilon_{l^+l^-}}{\mathrm{d}y\mathrm{d}p_t\mathrm{d}M}\left(T(x),\mu_i(x),\boldsymbol{v}(x)\right)\mathrm{d}^4x \tag{1}$$

where $\epsilon_{l^+l^-}$ denotes the rate of dileptons emitted per unit time and volume for a 4-momentum $p=(p_0,\boldsymbol{p})$ of the virtual photon of invariant mass $M=\sqrt{p^2}$; T, μ_i and $\boldsymbol{v}$ are the local temperature, chemical potentials and flow velocity of the medium. For a coarse-grained reaction volume the above expression reduces to a discrete sum

$$\left\langle \frac{\mathrm{d}N_{l^+l^-}}{\mathrm{d}y\mathrm{d}p_t\mathrm{d}M} \right\rangle = (\Delta x)^3\,\Delta t \sum_{k,l,m,t_j} \frac{\mathrm{d}\epsilon_{l^+l^-}}{\mathrm{d}y\mathrm{d}p_t\mathrm{d}M}\left(\langle T\rangle_{k,l,m,t_j},\langle\mu_i\rangle_{k,l,m,t_j},\langle\boldsymbol{v}\rangle_{k,l,m,t_j}\right) \tag{2}$$

where k,l,m label the cartesian coordinates x,y,z of a cubic spatial cell of volume $(\Delta x)^3$, j the time-step of duration Δt, and $\langle\cdot\rangle$ the ensemble average for a given cell.

The thermal emissivity can be expressed in standard form as

$$\frac{\mathrm{d}\epsilon_{l^+l^-}}{\mathrm{d}^4p} = \frac{\alpha_{EM}^2}{\pi^2M^2}\,f_B(p_0,T)\,\rho_{\mathrm{EM}}(M,p;T,\mu_i) \tag{3}$$

in terms of the EM spectral function $\rho_{\mathrm{EM}}=-\mathrm{Im}\Pi_{\mathrm{EM}}/\pi$ of the QCD medium (Π_{EM}: EM current-current correlation function) and the thermal Bose distribution function, f_B. The chemical potentials, μ_i, in Eq. (3) refer to the baryonic one (i=B), but also to effective meson chemical potentials (i=π, K) which build up in the space-time evolution of the thermal fireball after its chemical freeze-out (where, by definition, inelastic collisions cease). An over-population of pions ($\mu_\pi>0$) is especially important for ρ-meson and dilepton production [45], as it induces an additional overall fugacity factor $z_\pi^\kappa=\exp(\kappa\mu_\pi/T)$, in the emissivity, where κ characterizes the number of pions involved in the ρ (dilepton) production process, *e.g.*, κ=2 for $\pi\pi\to\rho$ or κ=1 for $\pi N\to\rho N$. We will return to this issue in Sec. 4 below.

In hadronic matter and in the low-mass region, $M\leq 1.1$ GeV, the vector dominance model directly relates the EM spectral function to the spectral functions of the light vector mesons, *e.g.*, $\mathrm{Im}\Pi_{\mathrm{EM}}=(m_\rho^4/g_\rho^2)\,\mathrm{Im}D_\rho$ for the dominant ρ-meson contribution. We account for the medium effects on the EM spectral function by employing a recently developed parameterization[1] of the ρ-meson spectral function calculated from hadronic many-body theory [45]. This spectral function is characterized by a strong broadening and ultimate "melting" of the ρ resonance in hot and dense hadronic matter; it provides a good description of all available low-mass dilepton data in ultrarelativistic heavy-ion collisions [15] (including the recently revised PHENIX data [13]), and of nuclear photo-production experiments [46, 47]. For practical use, the parameterization is provided in terms of the dilepton's mass (M) and 3-momentum (p), and as a function of temperature, pion and kaon chemical potentials as well as an effective baryon density defined as $\varrho_{\mathrm{eff}}=\varrho_N+\varrho_{\bar N}+1/2(\varrho_R+\varrho_{\bar R})$. Here $\varrho_{N(\bar N)}$ denotes the density of (anti-) nucleons and $\varrho_{R(\bar R)}$ of (anti-) baryon resonances (including both N^* and Δ states). The factor of $1/2$ for the latter is a conservative estimate, reflecting the finding that ρ-induced resonances on excited baryons are usually more weakly coupled (and/or less known) than for ρN scattering [45]. The contributions from anti-baryons are irrelevant in the SIS18 energy regime. This parameterization is generally accurate within a few tens of percent (better for space-time integrated spectra), which is sufficient for the purpose at hand. It has recently been deployed into a coarse-grained approach at SIS and SPS energies, resulting in good agreement with the measurements of HADES in Ar+KCl collisions and the high-precision NA60 data [39, 40] (which, in turn, also supports the viability of the coarse-graining procedure). We also include radiation from a hadronic

[1] The parametrization is available from one of the authors (RR) upon request. It is the same one as used in Refs. [39, 40].

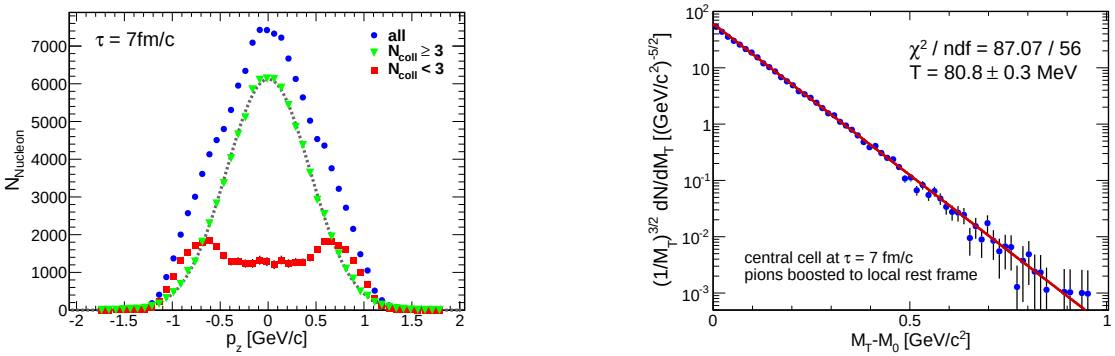

Fig. 1. (Color online) Left panel: Distribution of the longitudinal momentum of nucleons for the time step at 7 fm/c after initial nuclear impact in the central cell. The blue circles refer to all nucleons, while the red squares only include nucleons which have experienced less than three collisions. Nucleons which underwent three or more interactions are represented by the green triangles. The gray dotted line shows a Gaussian fit to this contribution. Right panel: M_T spectrum of pions in the central cell at the same time step at 7 fm/c (blue circles). The red line is an exponential fit to UrQMD "data" to extract a temperature.

continuum relevant for the intermediate-mass region (IMR; $M > 1$ GeV/c^2) using a standard parameterization deduced from the cross section for $e^+e^- \to$ hadrons annihilation [48],

$$\rho_{\rm EM}^{\rm cont}(M) = \frac{1}{4\pi^2}\left(1+\frac{\alpha_s}{\pi}\right)\frac{M^2}{1+\exp[(E_0-M)/\delta]}\ . \tag{4}$$

with a "threshold" energy E_0=1.5 GeV and width δ=0.2 GeV, and α_s =0.5. We here neglect medium effects, *e.g.*, due to chiral mixing, which are operative for $M < 1.5$ GeV, mostly because they are not material for our present purpose and because their assessment in baryon-rich matter is not straightforward.

3 Fireball Evolution

For the bulk evolution transport model we employ Ultra-relativistic Quantum Molecular Dynamics (UrQMD) [27] which successfully describes most of the hadron data in heavy-ion collisions at relativistic energies. We perform the coarse-graining following the approach of Ref. [38] by simulating an ensemble of heavy-ion collisions at fixed centrality at SIS18 energy. To optimize the conditions for the main assumption underlying the coarse-graining, we focus on the largest system available, *i.e.*, central Au+Au collisions at 1.23A GeV [2] beam energy on a stationary target, corresponding to $\sqrt{s_{NN}} = 2.4$ GeV. We discretize the spatial volume into 21^3 cubic cells of volume $\Delta x\Delta y\Delta z = 1\,{\rm fm}^3$ (covering 10.5 fm in each direction from the center) and analyze them in time steps of $\Delta t = 1$ fm/c. For each cell we determine an ensemble average over many events for the spatial momentum components p_x, p_y and p_z of each particle species, *i.e.*, pions, nucleons and $\Delta(1232)$. For the following discussion we divide the cells into two classes. We define an *inner cube* of cells covering a volume of $7^3 \times 1$ fm^3 around the collision center, and an *outer shell* containing in total $(21^3 - 7^3)$ fm^3.

We first illustrate how the longitudinal momentum distribution of the incoming nucleons, carrying the beam momentum, changes in the early stages between first impact and full overlap. In the center of the collision, after approx. 3 fm/c, a Gaussian distribution around $p_z = 0$ starts to build up from the nucleons which have collided three times or more. After 7 fm/c, this Gaussian component makes up ∼70% of the nucleons (see left panel of Fig. 1), indicating a remarkably rapid trend toward thermalization. Another measure to judge the degree of thermalization within the cells is the transverse-mass distribution for a given particle species, either $M_T^{-2}\,dN/dM_T$ at midrapidity or $M_T^{-3/2}\,dN/dM_T$ when integrated over all rapidities [49]. In case of thermalization the spectra will exhibit an exponential shape. The right panel of Fig. 1 shows that, after the nuclear penetration of 7 fm/c, pions are well described by a thermal M_T spectrum of temperature $T \simeq 80$ MeV.

Next, we extract the local cell temperatures as well as baryon and pion densities defined in the rest frame of the cells. We determine the rest frame by evaluating the baryon four-current for each cell which yields its collective velocity $\boldsymbol{v}_{klm}(t_j)$. This velocity is used to boost all hadron momenta into the cell's rest frame which readily yields its baryon (both nucleon and Δ) and pion density $\varrho_{i,\,klm}(t_j)$. The rest frame momenta of the different particles can then be used to fill properly normalized M_T spectra (as in the right panel of Fig. 1). The inverse slopes of exponential fits to the

[2] This particular beam energy has been chosen in view of the upcoming HADES results on Au+Au reactions taken at this energy.

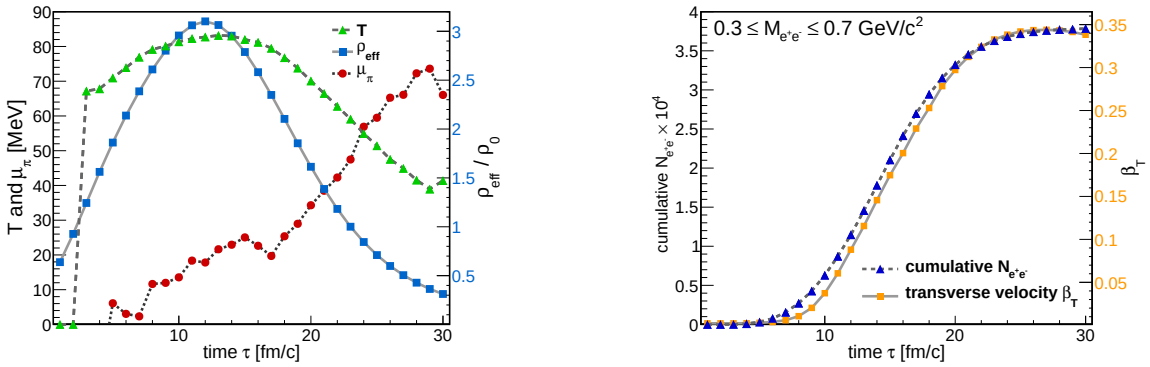

Fig. 2. (Color online) Left panel: Time evolution of the ensemble-averaged temperature extracted from pion M_T spectra (green triangles), effective baryon density (blue squares, right vertical scale in units of nuclear saturation density, ϱ_0=0.16 fm^{-3}) and pion chemical potential (red circles) averaged over the inner cube of 7^3 cells (each of volume 1 fm^3) around the collision center. Right panel: Time evolution of the cumulative radiated dilepton yield in the mass range $M = 0.3 - 0.7$ GeV/c^2 (blue triangles) and of the average collective transverse velocity in the outer shell of cells (orange squares, right vertical scale).

distributions of pions are used to define mean local temperatures $T_{klm}(t_j)$ for all cells and all time steps. Pions are our default choice for this purpose since they are strictly produced, the lightest hadrons and hence abundantly created and the key catalysts for producing dileptons. However, below we will discuss the uncertainty for dilepton production associated with this choice by also using nucleons. As it will turn out, the pions (nucleons) yield temperatures which are slightly lower (larger) than the method of using the energy density from an underlying equation of state in Ref. [40]. This result is not unexpected (since the EoS method in essence averages over all species), but it provides an error estimate for this central component of the coarse-graining procedure. With temperature and pion densities at hand, the pion chemical potential is determined through a fugacity factor z_π in Boltzmann approximation.

For simplicity, we omit the discretization indices in the following. The time evolution of the temperature, effective baryon density, $\varrho_{\rm eff} = \varrho_N + \frac{1}{2}\varrho_\Delta$, and pion chemical potential, averaged over the inner cube, are displayed in the left panel of Fig. 2. One finds the well-known result for these collisions energies [20] that the system evolves for a rather long duration of about 20(25) fm/c at baryon densities above (half) normal nuclear matter density. Maximal compression is reached after about 10-12 fm/c, and a maximal temperature of 75-85 MeV is maintained for approx. 10 fm/c around the maximal compression phase. A sizable pion chemical potential develops in the late stages of the fireball evolution. This is contrary to the coarse-graining results of Ref. [40], where μ_π starts out with a maximum close to maximum compression and then falls to zero over time. This discrepancy requires further studies. In the right panel of Fig. 2 we show the transverse collective expansion velocity (extracted from the baryon current) as seen by the outer shell of cells. It starts to develop slightly before maximal compression (but after full nuclear overlap) and lasts for a duration of ∼12-14 fm/c, until the baryon density has decreased to near nuclear saturation density.

4 Dilepton Spectra

The last ingredient needed to calculate dilepton spectra is the effective fugacity factor, z_π^κ, or more specifically, the effective pion number, κ, in the dilepton production processes at SIS18 energies. At ultrarelativistic energies it is routinely taken as κ=2, as the main production mechanism of the ρ-meson is via $\pi\pi$ annihilation. In Ref. [40] κ=2 was assumed also for SIS18 energies, although the situation for ρ production is somewhat different here. To account for this, we have extracted from UrQMD the individual production channels in order to asses how many pions are involved. The direct annihilation of two pions contributes ∼15%, while the dominant channel through baryon resonance decays amounts to ∼85%; UrQMD further allows to trace back the collision history to determine how many pions were involved in creating a resonance that subsequently decays into a ρ-meson. We find that ∼30% of these resonances are produced in NN collisions (0-π process), ∼50% with 1-π, ∼15% in 2-π processes and the remaining ∼5% with three or more pions. Thus the average number of pions creating a ρ amounts to κ = 1.12. We utilize this as our baseline average fugacity factor (and quantify the consequences when varying it below), in line with the philosophy of the coarse graining. For the continuum emission, eq. (4), the fugacity factor in a baryon-rich medium is much more difficult to determine (even in a meson-dominated medium it is non-trivial [14]). As it will turn out, the radiation in the IMR will be strongly dominated by the hottest phases where μ_π is small. We therefore neglect the fugacity factor for the continuum emission and comment on the impact of this approximation below.

We are now in position to evaluate Eq. (2) and to obtain the radiated dilepton spectra from the coarse-grained approach, using the local temperatures, effective baryon densities and pion chemical potentials in each cell for the

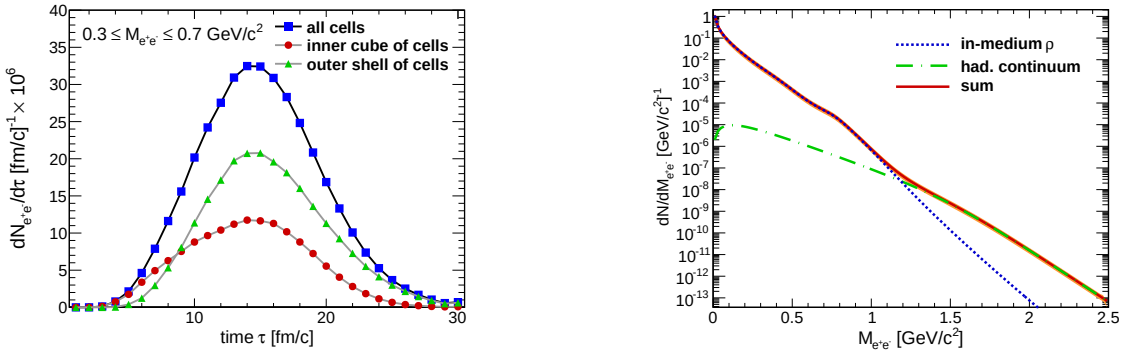

Fig. 3. (Color online) Left panel: Time evolution of the radiated dilepton yield per unit time in the mass range $M = 0.3 - 0.7$ GeV/c^2. The contribution of all cells together is shown by the blue squares, while the red circles (green triangles) display the share from the inner cube (outer shell) of cells. Right panel: Invariant-mass spectrum of e^+e^- pairs radiated from a central Au+Au collision at 1.23A GeV. The blue dotted line shows the contribution of the in-medium ρ-meson decays, while the green dotted-dashed lines represents the radiation from the hadronic continuum. The sum of both results in the red solid line which is drawn together with an orange error band of ±27%.

emissivity, Eq. (3). To begin with, we integrate (sum up) the 4-momentum differential spectrum, Eq. (2), over all 3-momenta and over a restricted mass window of $M = 0.3 - 0.7$ GeV/c^2. This window has been identified in a previous work [2] to yield a suitable measure of the lifetime of the interacting fireball. The time evolution of the cumulative dilepton yield in this window is displayed in the right panel of Fig. 2. Several interesting features emerge. First, the active radiation window of ∼13 fm/c (for $\tau \simeq$ 8-21 fm/c to produce 85% of the emission) very closely follows the build-up of the collective medium flow. Since collectivity is an explicit manifestation of the (thermal) pressure in the system, *i.e.*, its thermodynamic response is a consequence of the interactions in the system; its clear correlation with "thermal" dilepton radiation strongly supports our identification of a "fireball lifetime". Second, the radiation duration is quite different from the 20-25 fm/c that the inner cube spends above nuclear saturation density. In the radiation window, the baryon densities and temperatures of the inner cube are above $\varrho_{\rm eff} = 1.5\varrho_0$ and $T \simeq 70$ MeV.[3] Third, contributions from the "pre-equilibrium" phase of nuclear penetration, $\tau =$ 0-7 fm/c, are negligible, while the EM shining commences shortly thereafter. Note that the assumption of thermal equilibrium ("maximum entropy") in our calculations provides an upper estimate for the emission from the early phases. At the same time this assumption appears to be well satisfied during the radiation window (as discussed above), and also leads to a rather rapid and well-defined termination of the radiation, suggestive for a thermal freeze-out.

Next, we test the quantitative relation between fireball lifetime and thermal dilepton yield, normalized to the number of charged particles, as put forward in Ref. [2] for collider energies. As was done in there, we restrict the dilepton and charged-particle numbers to one unit around midrapidity. Unlike at larger energies, $\sqrt{s_{NN}} \gtrsim 5$ GeV, the fireball at lower energies is dominated by the incoming nucleons, not by the produced particles. In the low-energy limit, the number of charged particles (protons) is therefore not a good proxy for the thermal excitation energy in the system. Instead, we normalize the dilepton yield to the number of charged pions. With $N_{l^+l^-} = 2.9 \cdot 10^{-4}$ and $N_{\pi^\pm} = 17.1$ in central Au+Au collisions at $E_{\rm lab} = 1.23A$ GeV, one obtains $N_{l^+l^-}/N_{\pi^\pm} = 17.0 \cdot 10^{-6}$. Based on Fig. 3 in Ref. [2], this translates into a fireball lifetime of $\tau_{\rm fb} \simeq 14$ fm/c. On the other hand, if we renormalize the results in Fig. 3 of Ref. [2] to the number of charged pions, the proportionality factor to the lifetime changes to ∼1.45, *i.e.*, $N_{l^+l^-}/N_{\pi^\pm} \times 10^6 \simeq 1.45\tau_{\rm fb}$ (this includes the contribution of strong final-state decays, which are also included in the coarse-grained yields). In this case the extracted lifetime turns out to be ∼12 fm/c, not far from the ∼13 fm/c estimated as the "radiation window".

Let us quantify some of the uncertainties in the coarse-grained approach to calculate the dilepton yield $N_{e^+e^-}$, as arising from the conversion of the bulk properties in UrQMD into thermodynamic quantities. Instead of pions, one could use the nucleons to extract a local temperature from their rest frame M_T (restricted to the ones which have collided at least three times). This temperature reaches up to 110 MeV in the central cell and is in general up to 30% higher than the temperature extracted from the pion spectra. However, when using this temperature to determine the corresponding pion chemical potentials, much smaller values for the latter emerge (to obtain the same pion density). Employing the combination of "nucleon temperature" and the pertinent μ_π's in Eq. (3) leads to an increase of the dilepton yield, $N_{e^+e^-}$, by about 25%, which is much smaller than a factor of ∼4 which would arise if the fugacity factor

[3] Note that the 3-volume of the inner cube, with a "radius" (3.5 fm) of about half the system radius ($R_{\rm Au} \simeq 6.5$ fm), makes up only ∼10% of the total fireball volume. Nevertheless, the integrated contributions to the dilepton yield from the inner cube (∼40%) and the outer shell (∼60%) are quite comparable (see left panel of Fig. 3), with the former being characterized by a slightly broader emission time distribution than the latter.

z_π^κ were neglected in both calculations. The latter is thus not only physically well motivated but also considerably stabilizes our numerical results. We furthermore examine the uncertainty of the κ values which might turn out to be somewhat different in transport approaches other than UrQMD. When varying κ between 1 and 1.3 we find a difference of less than 10% in the low-mass dilepton yields compared to our default value.

Finally, we analyze the spectral shape of the calculated invariant-mass spectra of thermal dileptons, cf. right panel of Fig. 3 showing their decomposition into in-medium ρ-meson decays and the hadronic continuum. The strong medium effects on the ρ-meson lead to a remarkably structureless low-mass spectrum with only a slight bump remaining in the region of the vacuum ρ mass. The medium effects appear to be even stronger than in the NA60 spectrum for In+In at 158A GeV beam energy. This is in part due to the larger collisions system, the lower temperatures (which produce steeper slopes), and the increased medium effects induced by the higher baryon densities. As discussed above, a large part of the radiation in the 1.23A GeV Au+Au system emanates from densities above 2 times saturation density, with a large fraction of nucleons (which, in the calculation of the ρ spectral function, induce stronger medium effects than excited baryons). This is further augmented by the suppression of the emission from the dilute phases, apparently caused by the drop in temperature in the later stages which cannot be compensated by the increase in volume. In some sense the situation is similar to the IMR at full SPS energy, where the temperature sensitivity of the overall Bose factor strongly biases the emission to the early phases. Since the initial temperatures at SIS are roughly 3 times smaller than at SPS, one expects the predominance of early emission roughly at a factor of 3 smaller invariant masses, which suggests that the role of the $M > 1.2$ GeV/c^2 region at SPS shifts to $M > 0.4$ GeV/c^2 at SIS18. This is probably the reason for our finding that the dilute phases contribute little at SIS18.

As is well known, the spectral slope of dilepton invariant-mass spectra is an excellent thermometer of the fireball, unaffected by blue-shift effects due to the collective medium expansion. This is especially true if the EM spectral function does not (or only weakly) depend on temperature, so that the temperature dependence is solely residing in the thermal Bose factor. This is rather well satisfied in the IMR, where the vacuum spectral function, $\mathrm{Im}\,\Pi_{\mathrm{EM}}/M^2$, is essentially a constant with thermal corrections suppressed at order T^2/M^2. After integration over 3-momentum, the emissivity is then approximately proportional to $\mathrm{d}\epsilon_{l^+l^-}/\mathrm{d}M \propto (MT)^{3/2}\exp(-M/T)$. A fit to our calculated mass spectrum in the IMR for $M = 1.5-2.5$ GeV/c^2 yields an inverse-slope parameter of $T_{\mathrm{s}} = 88 \pm 5$ MeV, which coincides with the highest temperatures reached in the central cube of the fireball. This implies that the pertinent dilepton radiation is entirely dominated by the hottest (not earliest!) phases of the fireball evolution, well in line with the trend found in the ultrarelativistic regime when lowering the collision energy, cf. Fig. 2 in Ref. [2].[4] In addition, facilitated by the strong broadening of the ρ-meson in baryonic matter above saturation density, also the low-mass spectrum in 1.23A GeV Au+Au collisions exhibits a near-exponential shape. A fit to the mass window $M = 0.3-0.7$ GeV/c^2 yields an inverse slope parameter of $T_{\mathrm{s}} = 64 \pm 5$ MeV, reflecting emission from a broader range of fireball conditions (thus its potential to measure the lifetime). Since the exponential sensitivity of the Bose factor to temperature is reduced for smaller masses, the increasing volume of the cooling fireball compensates the thermal suppression for a while.

From the above findings the following picture of thermal dilepton radiation in heavy-ion collisions in the few-GeV regime emerges. In the early collision stages, the effect of the temperature in the system is compensated by the smallness of the active volume, *i.e.*, the build-up of entropy is not very fast and, as a consequence, the emitted radiation is negligible. This is a rather welcome feature as pre-equilibrium radiation is theoretically difficult to assess. We recall that the assumption of local equilibrium in the coarse-graining procedure provides an upper limit of the emitted radiation, at least for momenta and masses of the order of the temperature. Only after the compression (density) has reached about 80% of its maximum value (about 8 fm/c after initial impact, shortly after the nuclei have fully overlapped), dilepton radiation picks up rather rapidly. At that point, about 80% of the nucleons have undergone at least three collisions and have formed a Gaussian momentum distribution around midrapidity, suggestive for thermalization. Only about 1 fm/c thereafter, transverse collectivity develops in response to the earlier created thermodynamic pressure, further supporting the notion of local near-equilibrium. The radiation phase lasts for around 13 fm/c, until about 21 fm/c. This implies that in this regime the drop in temperature is compensated by the growing fireball volume, down to temperatures as high as ∼65 MeV in the central cube (somewhat lower in the outer shells). This is independently verified by the inverse-slope parameter of the low-mass dilepton spectrum. It further implies that there is little dilepton radiation from the stages with baryon densities around nuclear saturation density and below. The development of the collective flow also ceases in this regime (after all, cold nuclear matter at saturation has vanishing pressure).

Finally, we briefly compare our results with the features at ultrarelativistic collision energies. At top SPS energies UrQMD suggests the formation of densities of more than 10 ρ_0 [39], with extracted initial temperatures of up to 250 MeV (consistent with the inverse slopes in the intermediate-mass dilepton spectrum [2] or the naive picture that most of the entropy has been produced once the nuclei have fully overlapped, after about ∼1 fm/c). Due to the longitudinal Lorentz contraction, the fireball volume is quite small in this early stage, producing appreciable dilepton radiation mostly in the IMR. Only a small fraction of the low-mass dilepton yield emanates from this phase; most of

[4] We note that if we were to include a fugacity factor in the continuum emission, the magnitude of the pertinent dilepton yield could increase significantly (depending on the precise value of κ) while not affecting its slope.

the low-mass yield is radiated throughout the fireball evolution with effective baryon densities around ρ_0 (after all, the low-mass yield probes the lifetime of the fireball). On the other hand, in the SIS energy regime low-mass radiation is largely emitted during the time interval in which the highest baryon densities are reached, well above ρ_0. Thus the low-mass spectrum is more sensitive to the baryon driven in-medium modifications. The predicted almost complete flattening of the ρ spectral function leads to an almost exponential shape of the low-mass spectrum (recall the right panel of Fig. 3), which provides an additional thermometer characterizing the radiation-active medium in the few-GeV collision energy regime.

5 Conclusion and Outlook

In the present work we have investigated thermal dilepton production in the SIS18 energy regime using the coarse-graining approach to interface a microscopic transport description with (locally) thermal dilepton rates. For the former we used the well-established UrQMD model, while for the latter we employed (a parameterization of) an in-medium ρ spectral function that describes available dilepton data at ultrarelativistic energies. While this is not a new approach, we were able to extract some intriguing new insights, focusing on Au+Au collisions at $1.23A$ GeV bombarding energy. The radiation from the early pre-equilibrium phases during nuclear penetration turns out to be negligible, while the main radiation window lasts for only about 13 fm/c, quite a bit shorter than expectations based on the density evolution. The radiation window remarkably coincides with the build-up of transverse collectivity in the fireball, which establishes a strong correlation between hadronic and EM activity and supports the notion of a locally near-thermalized system (justifying the coarse-graining approach a posteriori). The correlation between collectivity and EM radiation could prove particularly useful in disentangling initial-state and collective effects in the current debate on p/d+A collisions at LHC and RHIC. Furthermore, we have investigated the relation between the system's lifetime and the low-mass dilepton excess yield and found it to follow the systematics put forward recently for ultrarelativistic collision systems. Finally we have extracted (blue-shift free) slope parameters and found that the intermediate-mass region remains an excellent thermometer for the hottest phase. In addition, thanks to the strong baryon-driven medium effects which essentially flatten the ρ line shape, the low-mass spectrum also becomes approximately exponential, providing an additional thermometer characterizing the conditions under which the bulk of the radiation is emitted. Altogether, our studies support the universality of dilepton spectra as a versatile probe of QCD matter formed in the fireballs of heavy-ion collisions over a broad range of energies.

6 Acknowledgements

This work was supported by the U.S. National Science Foundation under grant PHY-1306359, by the Humboldt foundation (Germany), by the Helmholtz-YIG grant VH-NG-823 at GSI and TU Darmstadt (Germany), and by the Hessian Initiative for Excellence (LOEWE) through the Helmholtz International Center for FAIR (HIC for FAIR).

References

1. R. Rapp, J. Wambach, and H. van Hees, Landolt-Bornstein **23** (2010) 134.
2. R. Rapp and H. van Hees, Phys. Lett. B**753** (2016) 586.
3. R. D. Pisarski, Phys. Lett. B**110** (1982) 155.
4. L. D. McLerran and T. Toimela, Phys. Rev. D**31** (1985) 545.
5. C. Gale and J. I. Kapusta, Nucl. Phys. B **357** (1991) 65.
6. S. Leupold, V. Metag, and U. Mosel, Int. J. Mod. Phys. E **19** (2010) 147.
7. P. M. Hohler and R. Rapp, Phys. Lett. B **731** (2014) 103.
8. G. Agakichiev *et al.* [CERES Collab.], Eur. Phys. J. C **41** (2005) 475.
9. R. Arnaldi *et al.* [NA60 Collab.], Phys. Rev. Lett. **96** (2006) 162302.
10. L. Adamczyk *et al.* [STAR Collab.], Phys. Rev. Lett. **113** (2014) 2, 022301.
11. L. Adamczyk *et al.* [STAR Collab.], Phys. Rev. C **92** (2015) 024912.
12. P. Huck *et al.* [STAR Collab.], Nucl. Phys. A **931** (2014) 659.
13. A. Adare *et al.* [PHENIX Collab.], Phys. Rev. C **93** (2016) 014904.
14. H. van Hees and R. Rapp, Nucl. Phys. A **806** (2008) 339.
15. R. Rapp, Adv.High Energy Phys. **2013** (2013) 148253.
16. T. Renk and J. Ruppert, Phys. Rev. C **77** (2008) 024907.
17. K. Dusling and I. Zahed, Phys. Rev. C **80** (2009) 014902.
18. G. Vujanovic *et al.* , Phys. Rev. C **89** (2014) 3, 034904.

19. J. Ruppert *et al.* , Phys. Rev. Lett. **100** (2008) 162301.
20. B. Friman (ed.) *et al.* , Lect. Notes Phys. **814** (2011) pp. 980.
21. M. Belkacem *et al.* , Phys. Rev. C **58** (1998) 1727.
22. A. Lang *et al.* , Z. Phys. A **340** (1991) 287.
23. G. Roche *et al.* [DLS Collab.], Phys. Lett. B **226** (1989) 228.
24. R. J. Porter *et al.* [DLS Collab.], Phys. Rev. Lett. **79** (1997) 1229.
25. G. Agakichiev *et al.* [HADES Collab.], Phys. Rev. C **84** (2011) 014902.
26. T. Galatyuk *et al.* [HADES Collab.], Nucl. Phys. A **931** (2014) 41.
27. S. A. Bass *et al.* , Prog. Part. Nucl. Phys. **41** (1998) 225.
28. J. Weil, H. van Hees, and U. Mosel, Eur. Phys. J. A **48** (2012) 111.
29. E. L. Bratkovskaya *et al.* , Phys. Rev. C **87** (2013) 6, 064907.
30. Gy. Wolf *et al.* , Nucl. Phys. A **517** (1990) 615.
31. Gy. Wolf, W. Cassing, and U. Mosel, Nucl. Phys. A **545** (1992) 139c.
32. M. Thomere, C. Hartnack, Gy. Wolf, and J. Aichelin, Phys. Rev. C **75** (2007) 064902.
33. O. Linnyk *et al.* , Phys. Rev. C **84** (2011) 054917.
34. B. Schenke and C. Greiner, Phys. Rev. C **73** (2006) 034909.
35. E. Santini, J. Steinheimer, M. Bleicher, and S. Schramm, Phys. Rev. C **84** (2011) 014901.
36. S. Damjanovic, Prog. Part. Nucl. Phys. **62** (2009) 381.
37. H. J. Specht *et al.* [NA60 Collab.], AIP Conf. Proc. **1322** (2010) 1.
38. P. Huovinen, M. Belkacem, P. J. Ellis, and J.I. Kapusta, Phys. Rev. C **66** (2002) 014903.
39. S. Endres, H. van Hees, J. Weil, and M. Bleicher, Phys. Rev. C **91** (2015) 054911.
40. S. Endres, H. van Hees, J. Weil, and M. Bleicher, Phys. Rev. C **92** (2015) 014911.
41. E. L. Bratkovskaya and W. Cassing, Nucl. Phys. A **807** (2008) 214.
42. O. Buss *et al.* , Phys. Rept. **512** (2012) 1.
43. H. Barz, B. Kampfer, Gy. Wolf, and M. Zetenyi, Open Nucl. Part. Phys. J. **3** (2010) 1.
44. Y. B. Ivanov, V. N. Russkikh, and V. D. Toneev, Phys. Rev. C **73** (2006) 044904.
45. R. Rapp and J. Wambach, Eur. Phys. J. A **6** (1999) 415.
46. M. H. Wood *et al.* [CLAS Collaboration], Phys. Rev. C **78** (2008) 015201.
47. F. Riek, R. Rapp, Y. Oh, and T.-S. H. Lee, Phys. Rev. C **82** (2010) 015202
48. E. V. Shuryak, Rev. Mod. Phys. **65** (1993) 1.
49. R. Hagedorn, Nuovo Cim. Suppl. **3** (1965) 147.